# Impact of Interbranch Correlation on Multichannel Spectrum Sensing with SC and SSC Diversity Combining Schemes

Salam Al-Juboori, *Student Member, IEEE,* Xavier Fernando, *SMIEEE,* Yansha Deng and A. Nallanathan *Fellow, IEEE,*
Department of Electrical and Computer Engineering, Ryerson University, Toronto, Canada
Department of Informatics, King's College London, London, WC2R 2LS, UK
School of Electronic Engineering and Computer Science, Queen Mary University of London, U.K
email: saljuboo@ryerson.ca, fernando@ee.ryerson.ca, yansha.deng@kcl.ac.uk, a.nallanathan@qmul.ac.uk

***Abstract*—Multi antenna receivers are often deployed in cognitive radio systems for accurate spectrum sensing. However, correlation among signals received by multiple antennas in these receivers is often ignored which yield unrealistic results. In this paper, the effect of this correlation is accurately quantified by deriving analytical expressions for the average probability of detection. Alternative simpler expressions are also derived. These are done for Selection Combining (SC) and Switch and Stay (SSC) diversity techniques in dual arbitrarily correlated Nakagami-$m$ fading channels. Then it is repeated for triple exponentially and identically correlated Nakagami-$m$ fading channels with SC diversity technique. Analysis results show that the inter-branch correlation impacts the detector performance significantly, especially in deep fading scenarios. Also, SC outperforms SSC as expected. However, the difference between them becomes very small in low fading and highly correlated scenarios which, indicates that the simpler SSC scheme can as well be deployed in such situations.**

***Index Terms*—Cognitive radio networks, spectrum sensing, inter-branch correlation, diversity combining, selection combining, switch and stay combining.**

## I. Introduction

PROTECTING the primary users from detrimental interference from the secondary user signals is crucial in cognitive radio systems. Accurate spectrum sensing is essential for this. Simple schemes such as Energy Detectors (ED) are widely used for this purpose that detect weak signals in noisy channels as long as the noise power is known [1]. Accurate spectrum sensing suffers from few issues, multipath fading and shadowing being the leading causes. Multi antenna receivers, with appropriate diversity combining schemes, are designed to overcome these issues. Ideally, wireless channels seen by the multiple antennas shall be independent to obtain the best results from these diversity receivers [2]. However, often this is not the case especially, when antennas are increasingly placed closer to each other as the mobile units get smaller and more demanding. Therefore, ignoring inter-branch correlation yields inaccurate, especially overly optimistic, results. The effects of multipath fading and correlation among antenna branches heavily depend on the type of the diversity combining technique employed. It is well known that Maximal Ratio Combining scheme (MRC) is the optimal scheme which is also the most complex linear diversity scheme. Equal Gain Combining (EGC) diversity technique is a close competitor. Both the MRC and EGC techniques require all or some knowledge of the Channel State Information (CSI) [3]–[5]. Furthermore, in these schemes each diversity branch must be equipped with a single receiver that increases the system complexity. Recently simpler combining schemes such as Switch and Stay Combining (SSC) and Selection Combining (SC) are getting popular due to their simplicity. These are especially useful in cognitive radio networks. With the SC scheme, the receiver simply selects the antenna with the highest received signal power and ignores other antennas. Hence, signal combiners, phase shifters or variable gain controllers are not required [3], [6]. The SSC diversity technique is the least complex system where no real combiner is required. The SSC selects a particular antenna branch until its SNR drops below a predetermined threshold [3]. Both SC and SSC schemes are required to measure only the amplitude on each branch (in order to select the highest one). Hence, they can be employed for both coherent and non-coherent modulation schemes [3]. Different diversity combining techniques have been studied in the literature. In [7], averaging the probability of detection over fading channels with Rayleigh, Nakagami-$m$ and Rician distributions are studied, and closed-form expressions for detector parameters were derived for Nakagami-$m$ channels with integer values of $m$. In [8]-[9], alternative analytic approaches to that in [1] and [7] were given. Furthermore, in [8], independent and identically distributed ($i.i.d$) dual and $L$ number of Rayleigh fading branches were considered with SSC and SC diversities. Corresponding average probability of detection expressions ($\overline{P}_D$) were also derived for both techniques. In [10]-[11], closed-form expressions for $\overline{P}_D$ were derived for $i.i.d.$ diversity branches in Nakagami-$m$ fading channels employing SC technique. In [12], closed-form expressions of $\overline{P}_D$ for $i.i.d$ dual Nakagami-$m$ fading branches with SSC were derived for real and integer $m$ values. In our previous work [6], we have done an investigation on the probability of detection for SC diversity with correlated Nakagami-$m$ fading branches. A review of prior works reveals that correlated fading branches with SSC diversity is not studied in the literature. However, because of the simplicity, the SSC is particularly valuable for mobile stations that have limited resource and power. This paper aims to fulfill that requirement.

In this paper, we extend our previous investigations by considering SC and SSC diversity combining techniques with identically correlated branches in Rayleigh and Nakagami-$m$ fading channels.

Our contribution falls into two folds. First

- We consider SC and SSC schemes with dual arbitrarily correlated branches in Rayleigh and Nakagami-$m$ fading channels.
- Then, we extend study of SC diversity to triple exponentially correlated branches.
- Corresponding novel expressions for average probability of detection are derived for each case.
- Alternative and more general and simpler expressions are also derived for each case.
- For SSC diversity, we derive an expression which can be solved numerically to calculate the optimal SNR threshold value in order to optimize the detector performance.
- All our derived expressions do converge rapidly.

Secondly, to gain better insight

- We do a performance comparison between the two combining diversity techniques
- Analysis results show that the inter-branch correlation affects the detector performance significantly, especially in deep fading scenarios.
- SC outperforms SSC as expected however; the difference between them becomes very small in low fading scenario with highly correlation among antennas. This indicates that the simpler SSC scheme can be substituted for the SC scheme in these situations.

The rest of the paper is organized as follows. Section II describes the system model. In section III, we study the performance of SC scheme. In section IV, we study the performance of SSC scheme. Section V describes simulation and analysis results. Section VI concludes the paper.

## II. System Model

We follow a binary hypothesis testing on the received signal to declare the presence or absence of the primary user. For this, we employ ED that is widely used in cognitive spectrum sensing. Note that no priori information about the detected signal is needed for ED [13], [14].

Let $x\,(t)$ be the received observations data

$$x\,(t) = h\,s\,(t) + n\,(t)\,, \tag{1}$$

where, $h$ is the complex channel gain amplitude coefficient, assumed to be constant during the sensing time, $s(t)$ is the signal to be detected and, $n(t)$ is the AWGN noise. This noise is a low-pass Gaussian process with zero mean and variance $N_0 W$ where, $N_0$ and $W$ denote Power Spectral Density (PSD) of the Gaussian noise and the signal bandwidth, respectively.

Two hypotheses are defined for the decision statistics. Namely $H_0$ and $H_1$, for the absence and the presence of the primary user signal respectively, as follows:

$$x\,(t) = \begin{cases} n\,(t) & under\ H_0 \\ h\,s\,(t) + n\,(t) & under\ H_1. \end{cases} \tag{2}$$

The decision statistics is squared and integrated over time $T$ at the ED. The output is written as

$$y \triangleq \frac{2}{N_0} \int_0^T |x|^2\,(t)\ \mathrm{d}t. \tag{3}$$

The Probability Density Function (PDF) of the decision statistics $y$ is given by [8] and [9]

$$p_Y\,(y) = \begin{cases} \frac{1}{2^u\,\Gamma(u)}\, y^{u-1}\, e^{-\frac{y}{2}}, & under\ H_0 \\ \frac{1}{2}\,\left(\frac{y}{2\,\gamma}\right)^{\frac{u-1}{2}}\, e^{-\frac{2\,\gamma+y}{2}}\, I_{u-1}\left(\sqrt{2\,\gamma\, y}\right), & under\ H_1 \end{cases} \tag{4}$$

where $\gamma$ denotes the signal-to-noise-ratio, $\Gamma(.)$ is the the Gamma function and, $I_\nu\,(.)$ is the $\nu^{\text{th}}$ order modified Bessel function of the first kind. The parameter $u$ depends on the time-bandwidth product. In (4), it is clear that the decision statistics has a central chi-square distribution with $2u$ degrees of freedom $\chi^2_{2u}$ in the absence of the primary user signal, i.e. the received samples are noise only. However, it has a non-central chi-square distribution $\chi^2_{2u}(\psi)$ with $2u$ degrees of freedom and non-centrality parameter $\psi = 2\gamma$ in the presence of the primary user signal [8] and [9].

Let us define $\lambda$ as the decision threshold. Then the probability of false alarm ($P_F$) and the probability of detection ($P_D$) of the ED can be written as

$$P_F = Pr\,(y > \lambda \mid H_0)\,, \tag{5}$$

$$P_D = Pr\,(y > \lambda \mid H_1)\,. \tag{6}$$

where $Pr\,(.)$ denotes the Cumulative Distribution Function (CDF). Consequently, the probability of false alarm and probability of detection in AWGN channel are given as [8] - [9]

$$P_F = \frac{\Gamma\left(u, \frac{\lambda}{2}\right)}{\Gamma(u)}, \tag{7}$$

$$P_D = Q_u\left(\sqrt{2\,\gamma},\, \sqrt{\lambda}\right), \tag{8}$$

where $\Gamma(.,.)$ and $Q_u\,(.,.)$ denote the upper incomplete Gamma function and generalized Marcum Q-function, respectively. These detection probabilities are conditioned upon the channel realization. Also, they represent *instantaneous* probability of detection. Therefore, we need to integrate this instantaneous probability of detection over the SNR's PDF of the corresponding fading channel ($p_{\gamma Div}\,(\gamma)$) to obtain the average probability of detection $\overline{P}_{D,Div}$[1].

$$\overline{P}_{D,Div} = \int_0^\infty Q_u\left(\sqrt{2\,\gamma},\, \sqrt{\lambda}\right) p_{\gamma Div}\,(\gamma)\, \mathrm{d}\gamma. \tag{9}$$

The expression in (9) will serve as a general expression for the corresponding diversity channel.

Note that the probability of detection expression in (8) is restricted to only integer values of $u$ since the PDF of the decision statistics in (4) is derived only for even numbers, i.e. $2u$, as stated in [8]. However, when the alternative Marcum-Q function is employed, $u$ could be half-odd integer

[1]False alarm probability is not a function of SNR as no signal is transmitted, therefore it will remain unchanged as in (7).

($u \in \{0.5, 1, 1.5, 2, 2.5, 3, ...\}$, i.e. not restricted to integer values) [15]. Furthermore, the fading parameter $m$ in Nakagami channels might also be not restricted to integer values depending on the mathematical method employed to solve the integral in (9). This highlights the advantage of the alternative expressions which we derive later using alternative Marcum-Q function.

## III. SC Diversity with Correlated Nakagami-$m$ fading Channels

In this section, we will derive the average probability of detection for dual and triple Nakagami-$m$ correlated fading branches with SC diversity.

Selection Combining is a low complexity diversity technique, as it chooses the highest SNR's branch using the relationship

$$r = \max\{r_l,\, l = 1,\, 2, \dots L\}\,. \tag{10}$$

Therefore it processes one branch a time. Consequently, no phase knowledge is required.

The PDF of a univariate $r$-Nakagami-$m$ variable is given by [16]

$$f_r\,(r) = \frac{2}{\Gamma(m)}\left(\frac{m}{\Omega}\right)^m r^{2\,m-1} e^{-\frac{m}{\Omega}r^2}, \quad r \geq 0 \tag{11}$$

where, $\Gamma(.)$ denotes the Gamma function, $\Omega = E[r^2]/m = \frac{\bar{r^2}}{m}$ is the mean value of the variable $r$, and $m$ ($m \geq 1/2$) is the inverse normalized variance of $r^2$, which describes the fading severity.

We define the instantaneous SNR per symbol per channel $\gamma_l$ as $\gamma_l = r_l^2 \frac{E_s}{N_0}$; $l \in [1,\, 2, \dots L]$; $E_s$ is the energy per symbol and, $N_0$ is the PSD of the Gaussian noise. The average SNR per branch is $\bar{\gamma}_l = \bar{r_l^2}\frac{E_s}{N_0}$ where, $\bar{r_l^2} = E[r_l^2]$ is the expectation of the channel envelop.

### A. SC with Dual arbitrarily Correlated Branches

Using [[17], Eq. (20)] and, by assuming identical diversity branches and by changing variables with some mathematical simplification, the PDF of the output SNR for a dual SC combiner under correlated Nakagami-$m$ fading channels can be obtained as

$$\begin{aligned} p_{\gamma SC}\,(\gamma) = {} & \frac{2}{\Gamma(m)}\left(\frac{m}{\bar{\gamma}}\right)^m \gamma^{m-1}\exp\left(\frac{-m\,\gamma}{\bar{\gamma}}\right) \\ & \times\left[1 - Q_m\left(\sqrt{2\,a\,\rho\,\gamma},\,\sqrt{2\,a\,\gamma}\right)\right], \quad \gamma \geq 0 \end{aligned} \tag{12}$$

where, $\rho$ denote the correlation coefficient between the two fading envelopes, and $a = \frac{m}{\bar{\gamma}\,(1-\rho)}$. Please see Appendix A for detailed derivation.

By substituting (12) into (9), the average probability of detection for dual correlated SC's diversity branches ($\overline{P}_{D,SC,2}$) is obtained as

$$\overline{P}_{D,SC,2} = \frac{2}{\Gamma(m)}\left(\frac{m}{\bar{\gamma}}\right)^m [I_A - I_B], \tag{13}$$

where

$$I_A = \int_0^\infty Q_u\left(\sqrt{2\gamma}, \sqrt{\lambda}\right)\gamma^{m-1}\exp\left(-\frac{m\gamma}{\bar{\gamma}}\right)\mathrm{d}\gamma, \tag{14}$$

and

$$\begin{aligned} I_B = \int_0^\infty & Q_u\left(\sqrt{2\gamma}, \sqrt{\lambda}\right) Q_m\left(\sqrt{2a\rho\gamma}, \sqrt{2a\gamma}\right) \\ & \times\gamma^{m-1}e^{-\frac{m\gamma}{\bar{\gamma}}}\mathrm{d}\gamma. \end{aligned} \tag{15}$$

Note this lengthy expression consists of two integrals, $I_A$ and $I_B$. We solve them separately. Please see Appendix B.

Hence, the average probability of detection for dual SC receiver under correlated identical Nakagami-$m$ fading branches (restricted to integer $u$ and $m$ values) is

$$\begin{aligned} \overline{P}_{D,SC,2} = {} & \frac{2}{\Gamma(m)}\left(\frac{m}{\bar{\gamma}}\right)^m \left[\frac{1}{2^{m-1}}\left\{G_1 + \frac{\eta}{2}\sum_{n=1}^{u-1}\frac{1}{n!}\left(\frac{\lambda}{2}\right)^n\right.\right. \\ & \left.\times{}_1F_1\left(m; n+1; \frac{\lambda\bar{\gamma}}{2\,(m+\bar{\gamma})}\right)\right\} - \sum_{n=0}^{\infty}\sum_{i=0}^{\infty}\sum_{k=0}^{i+m-1}\frac{\Gamma\left(u+n,\,\frac{\lambda}{2}\right)}{\Gamma(u+n)\;n!} \\ & \left.\times\,\frac{a^{i+k}\,\rho^i\,(i+k+m+n-1)!}{c^{i+k+m+n}i!\,k!}\right], \end{aligned} \tag{16}$$

where $c = \left(1 + a\,\,(\rho+1) + \frac{m}{\bar{\gamma}}\right)$ and $G_1$ for integer $m$ values is

$$\begin{aligned} G_1 = {} & \frac{2^{m-1}\,(m-1)!}{\left(\frac{m}{\bar{\gamma}}\right)^{2\,m}}\left(\frac{\bar{\gamma}}{m+\bar{\gamma}}\right)e^{-\frac{\lambda}{2}\,\frac{m}{m+\bar{\gamma}}} \\ & \times\left[\left(\frac{m+\bar{\gamma}}{\bar{\gamma}}\right)\left(\frac{m}{m+\bar{\gamma}}\right)^{m-1} L_{m-1}\left(-\frac{\lambda\,\bar{\gamma}}{2\,(m+\bar{\gamma})}\right)\right. \\ & \left.+\sum_{n=0}^{m-2}\left(\frac{m}{m+\bar{\gamma}}\right)^n L_n\left(-\frac{\lambda\,\bar{\gamma}}{2\,(m+\bar{\gamma})}\right)\right]. \end{aligned} \tag{17}$$

Here $L_n\,(.)$ denotes Laguerre polynomial of $n$-degree [18], and ${}_1F_1\,(.,.;.)$ denotes the Confluent Hypergeometric function. This is defined in [[19], Eq. (15.1.1)] as

$${}_1F_1\,(a_1, b_1; x) = \frac{\Gamma(b_1)}{\Gamma(a_1)}\sum_{i=0}^{\infty}\frac{\Gamma(a_1+i)\,x^i}{\Gamma(b_1+i)\,i!}. \tag{18}$$

Note (16) reduces to dual correlated Rayleigh fading branches for $m = 1$. It's worthwhile to mention that for $i.i.d.$ diversity branches, (16) reduces to [[9], Eq.(7), [8], Eq. (20)] multiplied by 2 (not exceeding unity)). The latter expression was derived for the average probability of detection in flat fading. Hence we have improved the detection performance and derived (16) to serve as a proof.

### B. Alternative Expression for $\overline{P}_{D,SC,2}$

Despite the fact that $Q_u\left(\sqrt{2\,\gamma},\,\sqrt{\lambda}\right)$ portion of the second integral $I_B$ in (13) is evaluated for $u$ values not-restricted to integer, (16) is still restricted to integer values. This is because, the first integral $I_A$ in (13) is only valid for integer $u$ and $m$ values. In this section, we derive a more general and simpler alternative expression for (16) that is not restricted to integer $u$ values. Please see Appendix C for the derivation.

$$\begin{aligned}\overline{P}_{D,SC,2} &= 1 - 2\left(\frac{m}{\bar{\gamma}}\right)^m e^{-\frac{\lambda}{2}} \\ &\times \Bigg[\frac{1}{d^m}\sum_{n=u}^{\infty}\left(\frac{\lambda}{2}\right)^n \frac{1}{\Gamma(n+1)}\,{}_1F_1\left(m; 1+n; \frac{\lambda}{2\,d}\right) \\ &- \frac{1}{\Gamma(m)}\sum_{n=u}^{\infty}\sum_{i=0}^{\infty}\sum_{k=0}^{i+m-1}\left(\frac{\lambda}{2}\right)^n \frac{\Gamma(m+i+k)a^{i+k}\rho^i}{\Gamma(n+1)c^{m+i+k}\, i!\, k!} \\ &\times {}_1F_1\left(m+i+k; 1+n; \frac{\lambda}{2\,c}\right)\Bigg].\end{aligned} \tag{19}$$

For $m = 1$, (19) reduces to the average probability of detection with dual correlated Rayleigh fading branches and, with $\rho = 0$ to $i.i.d$ dual Rayleigh fading branches given in ( [8], Eq. (30)).

Fortunately, the error resulting from truncating the infinite series in (19) is upper bounded by the Confluent Hypergeometric function defined in (18). Since this function is monotonically decreasing with $i, k$ and $n$ for given values of $m$, $\lambda$ and $\bar{\gamma}$ [20], the number of terms ($N_n$ and $N_i$) that required five digit accuracy could be calculated. These numbers are shown in Table I for different values of $\rho$ and $m$.

It's worthwhile to mention that several solutions for integrals involving the Marcum Q-function are available in literature [21]–[25]. However, our case of study in (15) solves a different and more complicated integral which involves a product of two Marcum Q-functions. These solutions are introduced in (57), (69) in Appendices B and C, respectively. To the best of knowledge, we believe that this solution is new in literature.

Finally, we'd like to mention that the solutions introduced in expressions (16) and (19) present a clear advantage over the numerical integration approach showed in (13) since a numerical integration is rather long and often gives approximated result. Furthermore, although expressions in (16) and (19) involve nested infinite series, they are either upper bounded by a monotonically decreasing confluent hypergeometric function or by an upper incomplete gamma function. Note that the latter could also be represented by a monotonically decreasing confluent hypergeometric function using [[28], Eq. (1.6)]. Consequently, these infinite series terms converge rapidly as we discussed earlier in Table I.

### C. SC with Triple Correlated Branches

In this section, we consider *triple* correlated diversity branches. We start from PDF of the fading envelope for trivariate Nakagami-$m$ channels given in [[26], Eq. (8)]. Then, by changing variable and by assuming identical branches ($\bar{\gamma} = \bar{\gamma_1} = \bar{\gamma_2} = \bar{\gamma_3}$, and the same fading parameter $m$), the PDF of the output SNR for triple SC exponentially correlated Nakagami-$m$ branches can be derived. This is shown below

$$\begin{aligned}p_{\gamma SC,3}(\gamma) = \frac{\left|\boldsymbol{\Sigma}^{-1}\right|^m}{\Gamma(m)}\sum_{i=0}^{\infty}\sum_{j=0}^{\infty}&\frac{\left|p_{1,2}\right|^{2\,i}\left|p_{2,3}\right|^{2\,j}}{p_{1,1}^{i+m}p_{2,2}^{i+j+m}p_{3,3}^{j+m}} \\ &\times\frac{[\Theta_1+\Theta_2+\Theta_3]}{\Gamma(m+i)\,\Gamma(m+j)\,i!\,j!},\end{aligned} \tag{20}$$

where $\boldsymbol{\Sigma}^{-1}$ is the inverse of the correlation matrix, $p_{i_1,j_1}(i_1, j_1 = 1,2,3)$ being its entries and $\Theta_1, \Theta_2$ and $\Theta_3$ are

$$\begin{aligned}\Theta_1 &= \left(\frac{p_{1,1}\,m}{\bar{\gamma}}\right)^{i+m}\gamma^{i+m-1}\,e^{-\frac{p_{1,1}\,m}{\bar{\gamma}}\gamma} \\ &\times\gamma\left(i+j+m, \frac{p_{2,2}\,m}{\bar{\gamma}}\gamma\right)\gamma\left(j+m, \frac{p_{3,3}\,m}{\bar{\gamma}}\gamma\right),\end{aligned} \tag{21}$$

$$\begin{aligned}\Theta_2 &= \left(\frac{p_{2,2}\,m}{\bar{\gamma}}\right)^{i+j+m}\gamma^{i+j+m-1}\,e^{-\frac{p_{2,2}\,m}{\bar{\gamma}}\gamma} \\ &\times\gamma\left(i+m, \frac{p_{1,1}\,m}{\bar{\gamma}}\gamma\right)\gamma\left(j+m, \frac{p_{3,3}\,m}{\bar{\gamma}}\gamma\right),\end{aligned} \tag{22}$$

$$\begin{aligned}\Theta_3 &= \left(\frac{p_{3,3}\,m}{\bar{\gamma}}\right)^{j+m}\gamma^{j+m-1}\,e^{-\frac{p_{3,3}\,m}{\bar{\gamma}}\gamma} \\ &\times\gamma\left(i+m, \frac{p_{1,1}\,m}{\bar{\gamma}}\gamma\right)\gamma\left(i+j+m, \frac{p_{2,2}\,m}{\bar{\gamma}}\gamma\right),\end{aligned} \tag{23}$$

respectively. Here $\gamma\,(a, x)$ denotes the lower incomplete gamma function with $\gamma(a,x) = \int_0^x e^{-t}\,t^{a-1}\,\mathrm{d}t$ ([18], Eq.(8.350/1)).

In exponentially correlated model, the diversity antennas are equispaced. Therefore, the correlation matrix can be written as $\Sigma_{i_1,j_1} \equiv \rho^{|i_1-j_1|}$ [27]. Hence, the inverse correlation matrix $\boldsymbol{\Sigma}^{-1}$ is tridiagonal and can be written as

$$\boldsymbol{\Sigma}^{-1} = \frac{1}{\rho^2-1}\begin{bmatrix}-1 & \rho & 0 \\ \rho & -(\rho^2+1) & \rho \\ 0 & \rho & -1\end{bmatrix}, \tag{24}$$

where $\rho$ denotes the correlation coefficient.

We have made an assumption of identical average SNRs in all three branches above. This assumption is reasonable if the diversity channels are closely spaced and, their gains as well as noise powers are equal [3].

The average probability of detection for triple SC diversity Nakagami-$m$ correlated branches with integer $u$ is derived as below. See Appendix D for details.

$$\begin{aligned}\overline{P}_{D,SC,3} &= \frac{\left|\boldsymbol{\Sigma}^{-1}\right|^m}{\Gamma(m)}e^{-\frac{\lambda}{2}}\sum_{n=0}^{\infty}\sum_{k=0}^{n+u-1}\sum_{i=0}^{\infty}\sum_{j=0}^{\infty} \\ &\Bigg[\left(\frac{\lambda}{2}\right)^k\left(\frac{\bar{\gamma}}{m}\right)^n\frac{\left|p_{1,2}\right|^{2\,i}\left|p_{2,3}\right|^{2\,j}}{p_{1,1}^{i+m}p_{2,2}^{i+j+m}p_{3,3}^{j+m}\Gamma(m+i)\Gamma(m+j)} \\ &\times\frac{p_{1,1}^{i+m}p_{2,2}^{i+j+m}p_{3,3}^{j+m}\Gamma(2i+2j+3m+n)}{\left(p_{11}+p_{2,2}+p_{3,3}+\frac{\bar{\gamma}}{m}\right)^{(2i+2j+3m+n)}\,i!j!k!n!} \\ &\times\left(\Xi_1+\Xi_2+\Xi_3\right)\Bigg].\end{aligned} \tag{28}$$

$$\Xi_1=\frac{F_2\left(2i+2j+3m+n;1,1;i+j+m+1,j+m+1;\frac{p_{2,2}}{p_{11}+p_{2,2}+p_{3,3}+\frac{\bar{\gamma}}{m}},\frac{p_{3,3}}{p_{11}+p_{2,2}+p_{3,3}+\frac{\bar{\gamma}}{m}}\right)}{(i+j+m)\,(j+m)}, \tag{25}$$

$$\Xi_2=\frac{F_2\left(2i+2j+3m+n;1,1;i+m+1,j+m+1;\frac{p_{1,1}}{p_{11}+p_{2,2}+p_{3,3}+\frac{\bar{\gamma}}{m}},\frac{p_{3,3}}{p_{11}+p_{2,2}+p_{3,3}+\frac{\bar{\gamma}}{m}}\right)}{(i+m)\,(j+m)}, \tag{26}$$

$$\Xi_3=\frac{F_2\left(2i+2j+3m+n;1,1;i+m+1,i+j+m+1;\frac{p_{1,1}}{p_{11}+p_{2,2}+p_{3,3}+\frac{\bar{\gamma}}{m}},\frac{p_{2,2}}{p_{11}+p_{2,2}+p_{3,3}+\frac{\bar{\gamma}}{m}}\right)}{(i+m)\,(i+j+m)}. \tag{27}$$

Here, $\Xi_1, \Xi_2$ and $\Xi_3$ are as given in (25), (26) and (27) at the top of next page, respectively, and $F_2\left(\alpha_3;\beta_3,\beta_3^{'};\gamma_3,\gamma_3^{'};x,y\right)$ denotes the Hypergeometric function of two variables defined in [[18], Eq. (9.180.2)]. Note, for $m=1$, (28) reduces to triple correlated Rayleigh fading branches.

### D. General Expression for Triple Branches

In this section, we will derive a general and simpler alternative expression to (28), where both $u$ and $m$ are not restricted to integer values. See Appendix E for details.

The average probability of detection for triple SC Nakagami-$m$ correlated branches for not restricted $u$ or $m$ integer values is:

$$\begin{aligned}\overline{P}_{D,SC,3}=&\frac{\left|\boldsymbol{\Sigma}^{-1}\right|^m}{\Gamma(m)}\sum_{n=0}^{\infty}\sum_{i=0}^{\infty}\sum_{j=0}^{\infty}\left(\frac{\bar{\gamma}}{m}\right)^n\frac{\Gamma\big(u+n,\frac{\lambda}{2}\big)}{\Gamma(u+n)}\\&\times\frac{|p_{1,2}|^{2\,i}\,|p_{2,3}|^{2\,j}\,\Gamma(2i+2j+3m+n)}{\Gamma(m+i)\,\Gamma(m+j)\,i!\,j!\,n!}\\&\times\frac{(\Xi_1+\Xi_2+\Xi_3)}{\left(p_{11}+p_{2,2}+p_{3,3}+\frac{\bar{\gamma}}{m}\right)^{2i+2j+3m+n}}.\end{aligned} \tag{29}$$

where $\Xi_1, \Xi_2$ and $\Xi_3$ are given in (25), (26) and (27), respectively. As before, for $m=1$, (29) reduces to triple correlated Rayleigh fading branches. It's worthwhile to mention that the Hypergeometric function of two variables $F_2\left(\alpha_3;\beta_3,\beta_3^{'};\gamma_3,\gamma_3^{'};x,y\right)$ appears in (28) and (29) converges only for $|x|+|y|<1$ [18], where $|.|$ denotes absolute. Fortunately, this is the case in our above derived equations.

## IV. Dual Correlated Nakagami-$m$ Channels with SSC Diversity

The SSC receiver selects a particular diversity branch until its SNR drops below a predetermined threshold value. Hence SSC's technique is similar to its counterpart SC but. Nevertheless, the SSC receive does not need to continuously monitor the SNR of each branch. Therefore, the SSC is considered as the least complex[2] diversity combining technique [3].

[2]Other diversity combining techniques such EGC and MRC process more than one branch and require the channel state knowledge of some or all the branches [3].

Starting from [[3], p.437, Eq. (9.334)], the SNR's PDF for a dual and identical correlated Nakagami-$m$ fading channels with SSC combiner is

$$p_{\gamma SSC}(\gamma)=\begin{cases}A(\gamma) & \gamma\le\gamma_T\\ A(\gamma)+\left(\frac{m}{\bar{\gamma}}\right)^m\frac{\gamma^{m-1}}{\Gamma(m)}\exp\left(-\frac{m\,\gamma}{\bar{\gamma}}\right) & \gamma>\gamma_T,\end{cases} \tag{30}$$

where $\gamma_T$ denotes a predetermined switching threshold and $A(\gamma)$ is given in [[3], p.437, Eq. (9.335)] as

$$\begin{aligned}A(\gamma)=&\left(\frac{m}{\bar{\gamma}}\right)^m\frac{\gamma^{m-1}}{\Gamma(m)}\exp\left(-\frac{m\,\gamma}{\bar{\gamma}}\right)\\&\times\left[1-Q_m\left(\sqrt{2\,a\,\rho\,\gamma},\,\sqrt{2\,a\,\gamma_T}\right)\right],\end{aligned} \tag{31}$$

where $a=\frac{m}{\bar{\gamma}\,(1-\rho)}$ and $Q_m(.,.)$ denotes generalized Marcum Q-function.

The average probability of detection for dual correlated Nakagami-$m$ fading branches with SSC diversity ($\overline{P}_{D,SSC,2}$) is obtained by substituting (30) into (9) and then using the definition $\int_a^\infty f\,\mathrm{d}x=\int_0^\infty f\,\mathrm{d}x-\int_0^a f\,\mathrm{d}x$, which yields

$$\overline{P}_{D,SSC,2}=\frac{1}{\Gamma(m)}\left(\frac{m}{\bar{\gamma}}\right)^m[I_A-I_B-I_C] \tag{32}$$

with

$$I_A=2\int_0^\infty Q_u\left(\sqrt{2\,\gamma},\,\sqrt{\lambda}\right)\gamma^{m-1}\exp\left(-\frac{m\,\gamma}{\bar{\gamma}}\right)\mathrm{d}\gamma, \tag{33}$$

$$\begin{aligned}I_B=&\int_0^\infty Q_u\left(\sqrt{2\,\gamma},\,\sqrt{\lambda}\right)Q_m\left(\sqrt{2\,a\,\rho\,\gamma},\,\sqrt{2\,a\,\gamma_T}\right)\\&\times\gamma^{m-1}\exp\left(-\frac{m\,\gamma}{\bar{\gamma}}\right)\mathrm{d}\gamma,\end{aligned} \tag{34}$$

and

$$I_C=\int_0^{\gamma_T} Q_u\left(\sqrt{2\,\gamma},\,\sqrt{\lambda}\right)\gamma^{m-1}\exp\left(-\frac{m\,\gamma}{\bar{\gamma}}\right)\mathrm{d}\gamma. \tag{35}$$

Before deriving an expression for the probability of detection $\overline{P}_{D,SSC,2}$, it is worthy to investigate (32) for the following two special cases of threshold values.

*Case* I: $\gamma_T=0$

If $\gamma_T=0$, we have $Q_m\left(\sqrt{2\,a\,\rho\,\gamma},\,\sqrt{2\,a\,\gamma_T}\right)=1$ and the third term $I_C$ vanishes, consequently (32) reduces to single branch detection as

$$\begin{aligned}\overline{P}_{D,SSC,2}=&\frac{1}{\Gamma(m)}\left(\frac{m}{\bar{\gamma}}\right)^m\int_0^\infty Q_u\left(\sqrt{2\,\gamma},\,\sqrt{\lambda}\right)\\&\times\gamma^{m-1}\exp\left(-\frac{m\,\gamma}{\bar{\gamma}}\right)\mathrm{d}\gamma.\end{aligned} \tag{36}$$

*Case* II: $\gamma_T \to \infty$
If $\gamma_T \to \infty$, we have $Q_m\left(\sqrt{2\,a\,\rho\,\gamma},\, \sqrt{2\,a\,\gamma_T}\right) = 0$, consequently $I_B$ vanishes and only $I_C$ is subtracted from $I_A$. This results in single branch detection as in (36). Therefore, care must be taken to choose a sensible threshold value. Otherwise, the diversity technique might become useless.

The average probability of detection for dual correlated SSC receiver with Nakagami-$m$ fading branches where $u$ and $m$ are restricted to integer values is given in (37) at the top of next page. Please see Appendix F for detailed derivation.

Note that for $m = 1$, (37) reduces to dual Rayleigh correlated fading branches, and for $\rho = 0$ it reduces to dual $i.i.d.$ Nakagami-$m$ fading branches detection.

### A. Alternative Solution

The expression $\overline{P}_{D,SSC,2}$ in (37) involves many infinite series representations. Some of their upper bounds (number of terms) are dependent on the preceded one. As an example the upper bound of the second sum ($\sum_{k=0}^{j+u-1}(.)$) depends on the number of terms $(N)$ needed for convergence of the previous series. Fortunately, it will not be very difficult to find the number of terms for convergence (with five digit accuracy). However, time for numerical implementation will be rather long. Therefore, we will derive an alternative more general and simpler expression $\overline{P}_{D,SSC,2}$ with less number of infinite series representations.

The average probability of detection where $u$ is not restricted while $(m \geq 1)$ is restricted to integer values is given in (38) at the top of next page. See Appendix G for the derivation.

Note, for $m = 1$, (38) reduces to that of a dual SSC receiver with Rayleigh correlated fading branches. For, $\rho = 0$ it reduces to the PDF of the dual $i.i.d.$ Nakagami-$m$ fading branches detection.

Interestingly, the three terms in (38) contain the upper incomplete gamma function in addition to the lower incomplete gamma function in the last term. In fact, we can represent both these functions by the monotonically decreasing confluent hypergeometric function using [[19], Eq. (6.5.12)] and [[28], Eq. (1.6)] for lower and upper incomplete gamma functions, respectively. Consequently the infinite series terms in (38) converges rapidly.

### B. Optimal Threshold ($\gamma_T^*$)

Optimal threshold $\gamma_T^*$ is defined as the value of the SNR that maximizes the probability of detection. We maximize the probability of detection by selecting an appropriate SNR for SSC switching. Probability of false alarm is fixed since it's a function of the decision threshold $\lambda$ and not a function of SNR, as shown in (7). Constant False Alarm Rate (CFAR) is a well-known technique that is often employed in cognitive spectrum sensing. In this technique and using (7), a decision threshold is calculated for fixed probability of false alarm. Then the corresponding probability of detection is calculated using (8) for optimal SNR. We have derived an expression for this optimal threshold given in (39) at the top of this page. This is done by differentiating $\overline{P}_{D,SSC,2}$ in (32) with respect to $\gamma_T$ and solving $\frac{\partial}{\partial \gamma_T^*}\overline{P}_{D,SSC,2} = 0$ for $\gamma_T^*$. See Appendix H for details. Using Matlab, we can obtain the optimal threshold by evaluating (39) numerically for $\frac{\partial}{\partial \gamma_T^*}\overline{P}_{D,SSC,2} = 0$.

Table I: Terms required for five digits accuracy

| $\overline{P}_{D,SC,2}$ : | $\tilde{E}_N$ , $u = 2, P_F = 0.01, \bar{\gamma} = 20$ dB | | | |
|---|---|---|---|---|
| $\rho$ | $m = 1$ $N_n, N_i$ | $m = 2$ $N_n, N_i$ | $m = 3$ $N_n, N_i$ | $m = 4$ $N_n, N_i$ |
| 0 | 15,1 | 15,1 | 15,1 | 15,1 |
| 0.2 | 15,3 | 15,3 | 15,2 | 15,1 |
| 0.4 | 15,3 | 15,2 | 15,1 | 15,1 |
| 0.6 | 15,3 | 15,5 | 15,4 | 15,4 |
| 0.8 | 15,4 | 15,5 | 15,6 | 15,7 |

## V. Simulation and Analysis Results

The energy detector employed in spectrum sensing is mainly characterized by the probability of false alarm $P_F$ and probability of detection $P_D$. In this section we study the impact of the correlation among antenna diversity branches on $P_D$ (equivalently probability of miss detection $P_{Dm} = 1 - P_D$ ) as a performance metric using the derived expressions in previous sections. To this end, we produce Complementary Receiver Operating Characteristic (CROC) graphs ($P_{Dm}$ versus $P_F$) for SC and SSC diversity techniques in Nakagami-$m$ fading channel.

First, we plot the probability of miss detection with the corresponding threshold $\lambda$ for $u = 2$, $\bar{\gamma} = 20$ dB, $m \in (1, 4)$ and, $\rho \in (0-0.8)$ for different values of $P_F$ using (7). Through Monte Carlo simulation, we obtain the CROC curves for SC and SSC. We then compare the simulation results with the analytical curves obtained from derived expressions.

In Figure. 1, we plot the CROC graphs for $L = 2, m = 1, \bar{\gamma} = 20$ dB and $\rho = 0.8$. Results are obtained for SC and SSC using both the derived expressions (analytical) and by Monte Carlo simulation. For SC diversity, both these curves are almost in a perfect match. However, reader may observe a very small difference between analytical and simulation curves for SSC diversity. This is due to the inaccuracy arising from rounding off the infinite series and calculating the optimal threshold .

In Figure 2, we plot the CROC graphs for SC with $\bar{\gamma} = 20$ dB, $m \in (1, 4)$ and, $\rho \in (0 - 0.8)$. For each value of fading severity $m$, one can clearly notice the degradation in the probability of detection due to the correlation among diversity branches. For instance, let us consider the case $m = 1$ and constant $P_F = 0.01$ as in Figure 2a. The corresponding $P_{Dm}$ for $\rho = 0.8$ is almost four times its value for $\rho = 0$ (no correlation). Similar result could be observed in Figure 2b, however, the increment ratio is now much more larger. However, as $m$ increases (low fading environment), correlation effect is compensated for, resulting in higher probability of detection (equivalently, low probability of miss detection). Thus, the rate of correlation compensation due to good channel is higher than the correlation impact on probability of detection.

For easy and better comparison between SC and SSC and their performance in combating the correlation, we plot CROC graphs in Figure 3 for $\bar{\gamma} = 20$ dB, $m \in (1, 4)$ and, $\rho \in (0, 0.8)$. As before, one can notice the impact of the correlation between fading branches on the probability of detection. This impact is

$$\overline{P}_{D,SSC,2} = \frac{1}{\Gamma(m)}\left(\frac{m}{\bar{\gamma}}\right)^{m} e^{-\frac{\lambda}{2}}\left[2\sum_{j=0}^{\infty}\sum_{k=0}^{j+u-1}\left(\frac{\lambda}{2}\right)^{k}\frac{(j+m-1)!}{j!\,k!}\left(\frac{\bar{\gamma}}{\bar{\gamma}+m}\right)^{j+m} - \sum_{n=0}^{\infty}\sum_{q=0}^{n+u-1}\sum_{i=0}^{\infty}\sum_{k=0}^{i+m-1}\left(\frac{\lambda}{2}\right)^{q} \right.$$
$$\left. \times \frac{a^{i+k}\,\rho^{i}\,(m+n+i-1)!}{\left(a\,\rho+\frac{m}{\bar{\gamma}}+1\right)^{m+n+i} i!\,k!\,n!\,q!}\; e^{-a\,\gamma_T}\,\gamma_T^{k} - \sum_{n=0}^{\infty}\sum_{q=0}^{n+u-1}\left(\frac{\lambda}{2}\right)^{q}\frac{1}{n!\,q!}\left(\frac{\bar{\gamma}}{\bar{\gamma}+m}\right)^{m+n}\gamma\left(m+n,\gamma_T\left(\frac{\bar{\gamma}+m}{\bar{\gamma}}\right)\right)\right] \tag{37}$$

$$\overline{P}_{D,SSC,2} = \frac{1}{\Gamma(m)}\left(\frac{m}{\bar{\gamma}}\right)^{m}\left[4\sum_{j=0}^{\infty}\frac{\Gamma\left(u+j,\frac{\lambda}{2}\right)\Gamma(m+j)}{\Gamma(u+j)\left(1+\frac{m}{\bar{\gamma}}\right)^{m+j} j!} - \sum_{n=0}^{\infty}\sum_{i=0}^{\infty}\sum_{k=0}^{i+m-1}\frac{\Gamma\left(u+n,\frac{\lambda}{2}\right)\Gamma(m+n+i)\,\gamma_T^{k}e^{-a\gamma_T}a^{i+k}\,\rho^{i}}{\Gamma(u+n)\left(\frac{m}{\gamma}+a\rho+1\right)^{m+n+i} n!\,i!\,k!}\right.$$
$$\left. - \sum_{p=0}^{\infty}\frac{\Gamma\left(u+p,\frac{\lambda}{2}\right)}{\Gamma(u+p)\,p!}\left(\frac{\bar{\gamma}+m}{\bar{\gamma}}\right)^{-(m+p)}\gamma\left(m+p,\gamma_T\left(\frac{\bar{\gamma}+m}{\bar{\gamma}}\right)\right)\right]. \tag{38}$$

$$\frac{\partial}{\partial\gamma_T^{*}}\overline{P}_{D,SSC,2} = \frac{1}{\Gamma(m)}\left(\frac{m}{\bar{\gamma}}\right)^{m}\left[\sqrt{2a\,\gamma_T^{*}}\,e^{-a\gamma_T^{*}}\sum_{k=0}^{\infty}\frac{a^{m+2k-1}\rho^{k}}{\Gamma(m+k)2^{m+k}\,k!}{\gamma_T^{*}}^{k}\left\{G_1^{'}+\frac{1}{2}\sum_{n=1}^{u-1}\left(\frac{\lambda}{2}\right)^{n}\frac{\Gamma\left(m+k\right)}{\left(\frac{a+1}{2}\right)^{m+k} n!}\right.\right.$$
$$\left.\left. \times\,{}_1F_1\left(m+k;n+1;\frac{\lambda}{2\,(a+1)}\right)\right\} - \;Q_u\left(\sqrt{2\,\gamma_T^{*}},\,\sqrt{\lambda}\right){\gamma_T^{*}}^{m-1}\exp\left(-\frac{m\,\gamma_T^{*}}{\bar{\gamma}}\right)\right]. \tag{39}$$

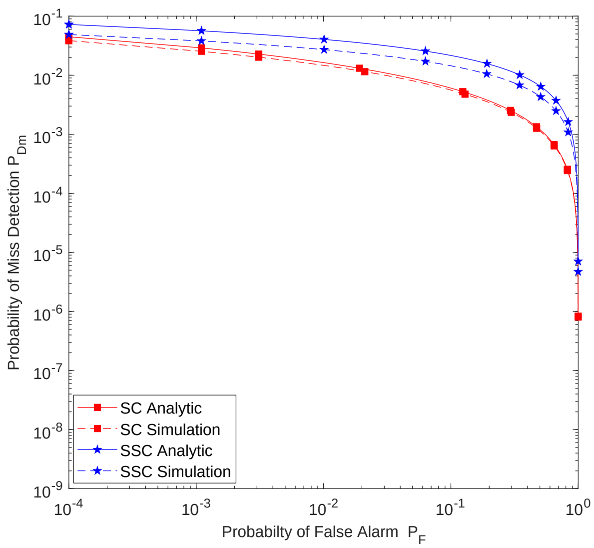


Figure 1: Analytic (solid) versus simulation (dashed) results for SC and SSC derived expressions with $L = 2, m = 1$, $\bar{\gamma} = 20$ dB and $\rho = 0.8$.

compensated by good channel. Furthermore, results in Figure 3 show that SC outperforms SSC. This is a well proven fact in the literature. In fact, performance difference is more pronounced for uncorrelated ($\rho = 0$) and high $m$ values. However, we may notice that as the correlation increases between the branches, the performance of both SC and SSC schemes becomes more comparable. This is especially true for high $m$ values.

Figure 4 shows probability of miss detection versus correlation for $\bar{\gamma} = 20$ dB, $m \in (1, 4)$ and, $P_F = 0.01$ for both SC and SSC diversity techniques. Another interesting behaviour that could be observed from this figure. As $m$ increases (equivalently, fading decreases), less significant deterioration in probability of detection is observed due to correlation. In other words, the loss in diversity gain due to correlation gets lower as $m$ increases.

To gain better insight about this behaviour, let us discuss it with more details. Figure 4a shows clearly this interesting behaviour. The curve for $m = 1$ in Figure 4a has an average high positive slope. Consequently, the probability of detection degrades rapidly as correlation increases. As $m$ increases, corresponding curves get flattened (slope decreases). Consequently, probability of detection degrades slowly as correlation increases. This can be attributed to the fact that already the $P_D$ values are high due to low fading. On the other hand, for small $m$-values (deep fading), correlation significantly deteriorates the probability of detection which is already poor. A similar behaviour could be observed in the SSC shown in Figure 4b. Therefore, we conclude the following. In a deep fading scenario, the inter-branch correlation is a crucial factor and its effects must be incorporated in any spectrum sensing model. By contrast, in a low fading environment (those having large values of $m$), the effect of such correlation may be ignored without much impact.

## VI. Conclusion

In this work, we have investigated the impact of correlation among diversity fading branches in multi-antenna cognitive radio spectrum sensing networks. A unified performance analysis was presented for the probability of detection of SC and SSC diversity combining receivers with arbitrary and exponential correlation among fading branches. Exact expressions were derived for the probability of detection for each case. Our result show that the correlation among diversity

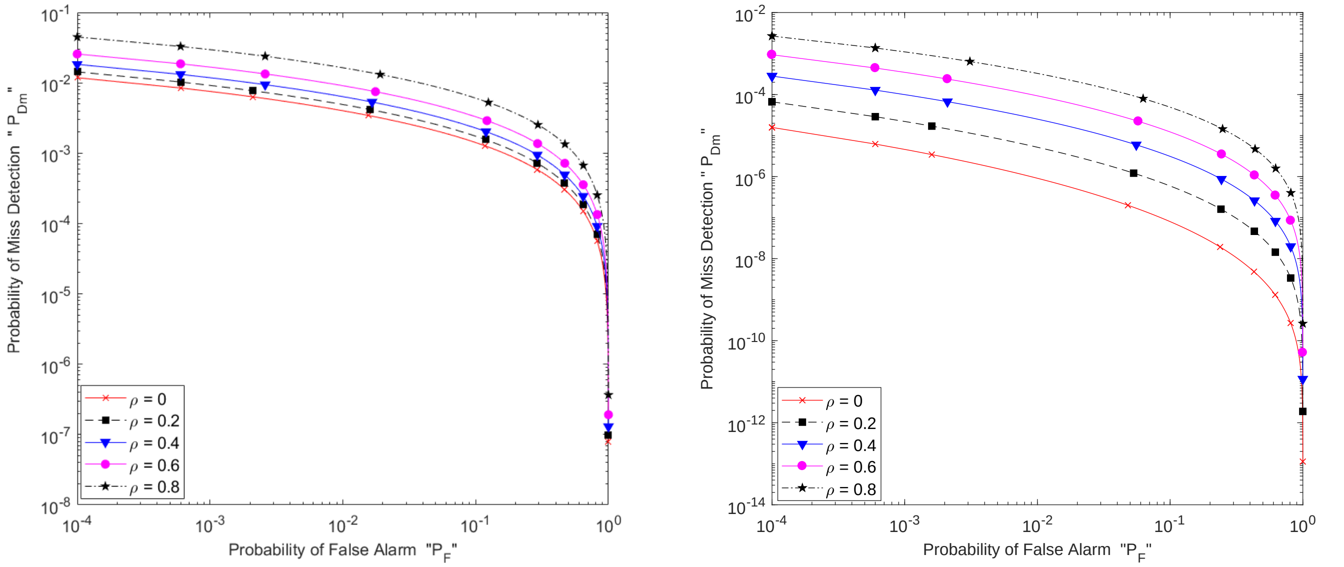


(a) $m = 1$ (Rayleigh) (b) $m = 4$

Figure 2: SC dual correlated Nakagami-$m$ branches with $\bar{\gamma} = 20$ dB for different $\rho$ values.

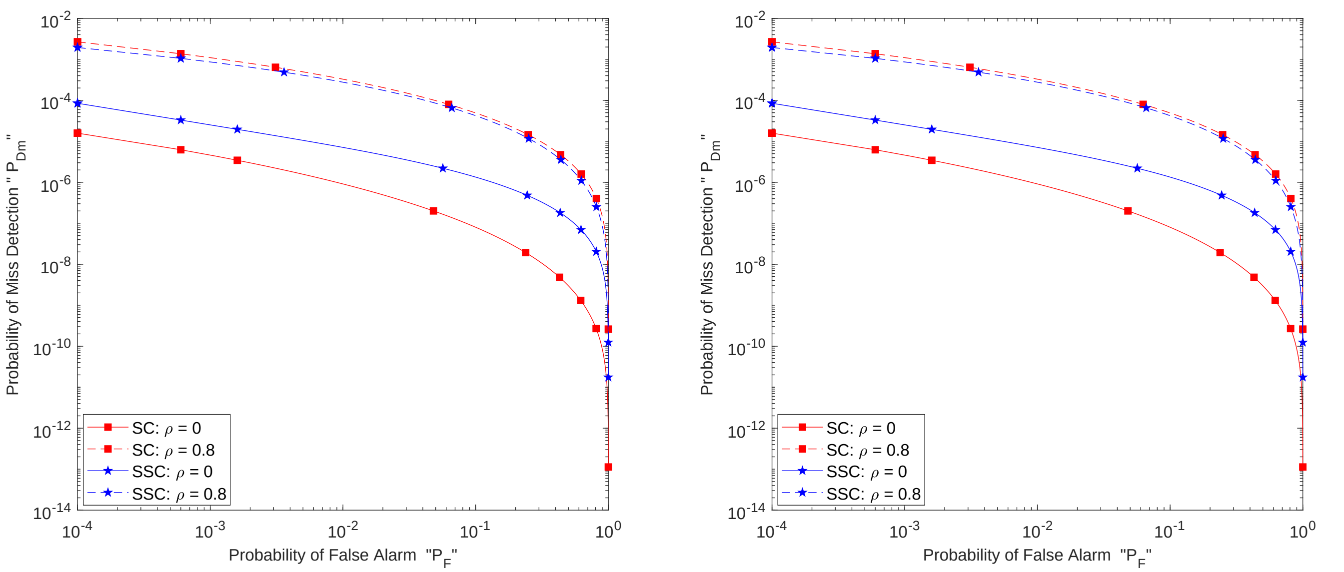


(a) $m = 1$ (Rayleigh) (b) $m = 4$

Figure 3: SC/SSC dual correlated Nakagami-$m$ branches comparison with $\bar{\gamma} = 20$ dB for $\rho = 0$ (solid) and $0.8$ (dashed).

fading branches causes an adverse impact on the probability of detection, which cannot be ignored especially under severe fading conditions. Consequently, an increase in the interference rate between the primary user and secondary user is observed by three times its rate when independent fading branches is assumed. Our investigations reveal that for low fading environment (large $m$-values), correlation effect may be ignored. Furthermore, at low fading and highly correlated environments, SSC which is simpler scheme performs as good as SC which is a more complex scheme.

## Appendix A
## Derivation of (12)

Using ([17], (20)), the PDF of SC's output of dual identical correlated Nakagami fading branches is

$$p_{\gamma SC}(r) = \frac{4\, m^m\, r^{2m-1}}{\Gamma(m)\Omega^m} \exp\left(-\frac{m\, r^2}{\Omega}\right) \times \left[1 - Q_m\left(\sqrt{2\,\rho} A\, r, \sqrt{2}\, A\, r\right)\right], \tag{40}$$

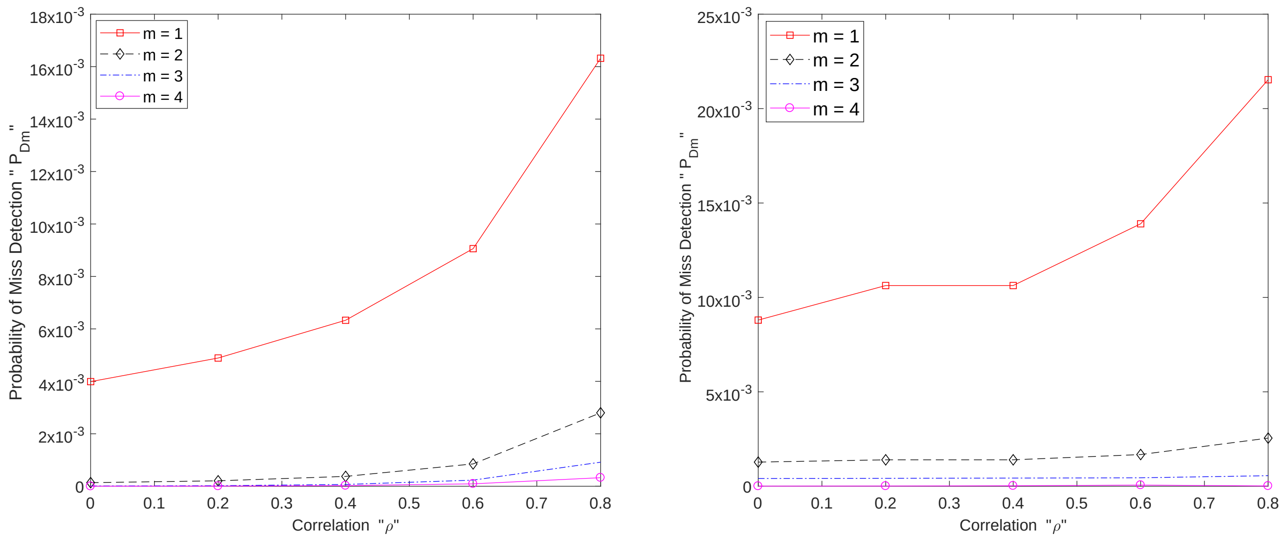


(a) SC (b) SSC

Figure 4: Probability of miss detection versus correlation with $\bar{\gamma} = 20$ dB, $P_F = 0.01$ and different fading severity for SC and SSC.

where $A = \sqrt{\frac{m}{\Omega(1-\rho)}}$.

Changing variables using $p_\gamma(\gamma) = \frac{p_r\left(\sqrt{\frac{\Omega\gamma}{\bar{\gamma}}}\right)}{2\left(\sqrt{\frac{\bar{\gamma}\gamma}{\Omega}}\right)}$ [3] yields

$$p_{\gamma SC}(\gamma) = \frac{4\, m^m \left(\sqrt{\frac{\Omega\,\gamma}{\bar{\gamma}}}\right)^{2m-1}}{2\left(\sqrt{\frac{\bar{\gamma}\,\gamma}{\Omega}}\right)\Gamma(m)\Omega^m} \exp\left(-\frac{m\left(\sqrt{\frac{\Omega\,\gamma}{\bar{\gamma}}}\right)^2}{\Omega}\right) \times \left[1 - Q_m\left(\sqrt{2\,\rho}A\sqrt{\frac{\Omega\,\gamma}{\bar{\gamma}}}, \sqrt{2}A\sqrt{\frac{\Omega\,\gamma}{\bar{\gamma}}}\right)\right], \tag{41}$$

Simplifying, (41) becomes

$$p_{\gamma SC}(\gamma) = \left(\sqrt{\frac{\Omega}{\bar{\gamma}\,\gamma}}\right) \frac{2\, m^m \left(\sqrt{\frac{\Omega\,\gamma}{\bar{\gamma}}}\right)^{2m-1}}{\Gamma(m)\Omega^m} \exp\left(-\frac{m\,\gamma}{\bar{\gamma}}\right) \times \left[1 - Q_m\left(\sqrt{2\rho}A\sqrt{\frac{\Omega\gamma}{\bar{\gamma}}}, \sqrt{2}A\sqrt{\frac{\Omega\gamma}{\bar{\gamma}}}\right)\right], \tag{42}$$

Substituting $A = \sqrt{\frac{m}{\Omega(1-\rho)}}$ and simplifying, yields

$$p_{\gamma SC}(\gamma) = \frac{\Omega^{1/2+m-1/2}}{\bar{\gamma}^{1/2}\gamma^{1/2}} \frac{2\, m^m\, \gamma^{m-1/2}}{\Gamma(m)\bar{\gamma}^{m-1/2}\Omega^m} \exp\left(-\frac{m\,\gamma}{\bar{\gamma}}\right) \left[1 - Q_m\left(\sqrt{2\rho}\sqrt{\frac{m}{\Omega(1-\rho)}}\sqrt{\frac{\Omega\gamma}{\bar{\gamma}}}, \sqrt{2}\,\sqrt{\frac{m}{\Omega(1-\rho)}}\,\sqrt{\frac{\Omega\,\gamma}{\bar{\gamma}}}\right)\right], \tag{43}$$

Simplifying

$$p_{\gamma SC}(\gamma) = \frac{2\, m^m}{\Gamma(m)\bar{\gamma}^m}\, \gamma^{1-m} \exp\left(-\frac{m\,\gamma}{\bar{\gamma}}\right) \times \left[1 - Q_m\left(\sqrt{\frac{2\, m\rho}{\bar{\gamma}(1-\rho)}\gamma}, \sqrt{\frac{2\, m}{\bar{\gamma}(1-\rho)}\gamma}\right)\right] \tag{44}$$

Simplifying and rearranging, this concludes the derivation.

## Appendix B
## Expression for Dual SC

In this appendix, we derive the expression in (16).

*1) Evaluating $I_A$ in (14):* Introducing changing variable $x = \sqrt{2\,\gamma}$, we can derive

$$I_A = \frac{1}{2^{m-1}} \underbrace{\int_0^\infty Q_u\left(x, \sqrt{\lambda}\right) x^{2\,m-1} \exp\left(-\frac{m\, x^2}{2\,\bar{\gamma}}\right) \mathrm{d}x}_{I}. \tag{45}$$

Using [[29], Eq. (29)], we write

$$\int_0^\infty Q_u\left(\alpha\, x, \beta\right) x^q\, e^{-\frac{p^2 x^2}{2}}\, \mathrm{d}x \equiv G_u = G_{u-1} + \frac{\Gamma\left(\frac{q+1}{2}\right)\left(\frac{\beta^2}{2}\right)^{u-1} e^{-\frac{\beta^2}{2}}}{2\,(u-1)!\left(\frac{p^2+\alpha^2}{2}\right)^{\frac{q+1}{2}}} \times {}_1F_1\left(\frac{q+1}{2}; u; \frac{\beta^2}{2}\,\frac{\alpha^2}{p^2+\alpha^2}\right), \quad q > -1, \tag{46}$$

we can solve $I$ by evaluating $G_u$ recursively for $q > -1$ and restricted $u$ integer values as

$$\begin{aligned} G_u &= G_{u-1} + A_{u-1}\, F_u \\ &= G_{u-2} + A_{u-2}\, F_{u-2} + A_{u-1}\, F_{u-1} \\ &\vdots \\ &= G_1 + \sum_{n=1}^{u-1} A_n\, F_{n+1}. \end{aligned} \tag{47}$$

where $A_n$ and $F_n$ are given as

$$A_n = \frac{1}{2\,(n!)\left(\frac{p^2+\alpha^2}{2}\right)^{\frac{q+1}{2}}} \Gamma\!\left(\frac{q+1}{2}\right)\left(\frac{\beta^2}{2}\right)^n e^{-\frac{\beta^2}{2}}, \tag{48}$$

$$F_n = {}_1F_1\left(\frac{q+1}{2}; n; \frac{\beta^2}{2}\,\frac{\alpha^2}{p^2+\alpha^2}\right), \tag{49}$$

and ${}_1F_1\,(.,.;.)$ as defined previously in (18). Hence, we solve (45) to obtain

$$\begin{aligned} I_A = \frac{1}{2^{m-1}} \Bigg[ G_1 + \frac{\eta}{2} \sum_{n=1}^{u-1} \frac{1}{n!}\left(\frac{\lambda}{2}\right)^n \\ \times {}_1F_1\left(m; n+1; \frac{\lambda\,\bar{\gamma}}{2\,(m+\bar{\gamma})}\right)\Bigg], \end{aligned} \tag{50}$$

where $\eta = \Gamma(m)\left(\frac{2\,\bar{\gamma}}{m+\bar{\gamma}}\right)^m e^{-\frac{\lambda}{2}}$ and $G_1$ can be obtained by evaluating the following integral containing the first order of Marcum $Q$-function $Q(.,.)$ for integer $m$ values as

$$G_1 = \int_0^\infty Q\left(x, \sqrt{\lambda}\right) x^{2\,m-1}\, e^{-\frac{m\,x^2}{2\,\bar{\gamma}}}\, \mathrm{d}x. \tag{51}$$

Using [[29], Eq. (25)], we evaluate $G_1$ for integer $m$ values as in (17).

*2) Evaluating $I_B$ in (15):* Using the alternative canonical Marcum Q-function representations for $Q_u\left(\sqrt{2\,\gamma},\, \sqrt{\lambda}\right)$ given in [15] for not restricted to integer values of $u$ as

$$Q_u\left(\sqrt{2\,\gamma},\, \sqrt{\lambda}\right) = \sum_{n=0}^{\infty} \frac{\gamma^n\, e^{-\gamma}\, \Gamma\!\left(u+n, \frac{\lambda}{2}\right)}{\Gamma(u+n)\; n!}, \tag{52}$$

and the alternative representation given in [[3], Eq. (4.74)] for restricted $m$ integer values as

$$\begin{aligned} Q_m\left(\alpha_1,\, \beta_1\right) = \sum_{i=0}^{\infty} \exp\left(-\frac{\alpha_1^2}{2}\right) \frac{\left(\frac{\alpha_1^2}{2}\right)^i}{i!} \\ \times \sum_{k=0}^{i+m-1} \exp\left(-\frac{\beta_1^2}{2}\right) \frac{\left(\frac{\beta_1^2}{2}\right)^k}{k!}, \end{aligned} \tag{53}$$

therefore, $Q_m\left(\sqrt{2\,a\,\rho\,\gamma},\, \sqrt{2\,a\,\gamma}\right)$ could be written as

$$Q_m\left(\sqrt{2a\rho\gamma}, \sqrt{2\,a\gamma}\right) = \sum_{i=0}^{\infty} \sum_{k=0}^{i+m-1} \frac{a^{i+k}\rho^i}{i!k!} e^{-a\gamma(\rho+1)}\gamma^{i+k}. \tag{54}$$

Then by substituting (52) and (54) into (15) with some simplification we derive

$$\begin{aligned} I_B = \sum_{n=0}^{\infty}\sum_{i=0}^{\infty}\sum_{k=0}^{i+m-1} \frac{\Gamma\!\left(u+n, \frac{\lambda}{2}\right)}{\Gamma(u+n)\; n!} \frac{a^{i+k}\,\rho^i}{i!\,k!} \\ \times \underbrace{\int_0^\infty \gamma^{i+k+m+n-1} e^{-\gamma c} \mathrm{d}\gamma,}_{I} \end{aligned} \tag{55}$$

where $c = 1 + a\,(\rho+1) + \frac{m}{\bar{\gamma}}$. Now the next task is solving the integral $I$ in (55). For this we use [[18], Eq. (3.351/3)] and satisfying the condition therein,

$$\int_0^\infty x^{p_1}\, e^{-\mu_1\, x}\, \mathrm{d}x = p_1!\, {\mu_1}^{-p_1-1} \quad [\mathrm{Re}\, \mu_1 > 0]\,. \tag{56}$$

Hence (55) becomes

$$I_B = \sum_{n=0}^{\infty}\sum_{i=0}^{\infty}\sum_{k=0}^{i+m-1} \frac{\Gamma\!\left(u+n, \frac{\lambda}{2}\right)}{\Gamma(u+n)} \frac{(i+k+m+n-1)!a^{i+k}\rho^i}{c^{i+k+m+n} n!\, i!\, k!} \tag{57}$$

Substituting (50) and (57) into (13), this concludes the derivation.

## Appendix C
## Alternative Expression for Dual SC

In this Appendix, we derive (19). Using the alternative expression for Marcum Q-function given in [[3], Eq.(4.63)], where $u$ is not restricted to integer values, we can write $Q_u\left(\sqrt{2\,\gamma},\, \sqrt{\lambda}\right)$ as

$$Q_u\left(\sqrt{2\gamma}, \sqrt{\lambda}\right) = 1 - e^{-\frac{2\gamma+\lambda}{2}} \sum_{n=u}^{\infty} \left(\frac{\sqrt{\lambda}}{\sqrt{2\gamma}}\right)^n I_n\left(\sqrt{2\lambda\gamma}\right). \tag{58}$$

Then substituting (12) in (9) and using the definition of the PDF as

$$\int_0^\infty p_\gamma\,(\gamma)\; \mathrm{d}\gamma = 1, \tag{59}$$

with simplification, we can derive

$$\overline{P}_{D,SC,2} = 1 - [I_A - I_B], \tag{60}$$

where

$$\begin{aligned} I_A = \frac{2}{\Gamma(m)}\left(\frac{m}{\bar{\gamma}}\right)^m \int_0^\infty \gamma^{m-1} e^{-\frac{2\,\gamma+\lambda}{2}} \sum_{n=u}^{\infty}\left(\frac{\sqrt{\lambda}}{\sqrt{2\,\gamma}}\right)^n \\ \times I_n\left(\sqrt{2\,\lambda\,\gamma}\right)\, \exp\left(\frac{-m\,\gamma}{\bar{\gamma}}\right)\mathrm{d}\gamma, \end{aligned} \tag{61}$$

and

$$\begin{aligned} I_B = \frac{2}{\Gamma(m)}\left(\frac{m}{\bar{\gamma}}\right)^m \int_0^\infty \gamma^{m-1} e^{-\frac{2\gamma+\lambda}{2}} \sum_{n=u}^{\infty}\left(\frac{\sqrt{\lambda}}{\sqrt{2\gamma}}\right)^n \\ \times I_n\left(\sqrt{2\lambda\gamma}\right) \exp\left(\frac{-m\gamma}{\bar{\gamma}}\right) Q_m\left(\sqrt{2a\rho\gamma}, \sqrt{2a\gamma}\right)\mathrm{d}\gamma,\ \gamma \geq 0. \end{aligned} \tag{62}$$

*1) Evaluating $I_A$ in (61):* Simplifying and rearranging (61), we derive

$$I_A = \frac{2}{\Gamma(m)} \left(\frac{m}{\bar{\gamma}}\right)^m e^{-\frac{\lambda}{2}} \sum_{n=u}^{\infty} \left(\frac{\lambda}{2}\right)^{\frac{n}{2}} \times \int_0^{\infty} \gamma^{m-\frac{n}{2}-1} e^{-\gamma\left(1+\frac{m}{\bar{\gamma}}\right)} I_n\left(\sqrt{2\lambda\gamma}\right) \mathrm{d}\gamma. \tag{63}$$

Using [[18], Eq. (6.643/2)] given as

$$\int_0^{\infty} x^{\mu-\frac{1}{2}} e^{-\alpha x} I_{2\nu}\left(2\beta\sqrt{x}\right) \mathrm{d}x = \frac{\Gamma\left(\mu+\nu+\frac{1}{2}\right)}{\Gamma(2\nu+1)} \beta^{-1} e^{\frac{\beta^2}{2\alpha}} \alpha^{-\mu} M_{-\mu,\nu}\left(\frac{\beta^2}{\alpha}\right), \left[Re\left(\mu+\nu+\frac{1}{2}\right) > 0\right], \tag{64}$$

where $M_{\mu,\nu}(.)$ denotes Whittaker function given by [18]

$$M_{\mu,\nu}(z) = z^{\nu+\frac{1}{2}} e^{-\frac{z}{2}} {}_1F_1\left(\nu-\mu+\frac{1}{2}; 1+2\nu; z\right), \tag{65}$$

with some simplification and rearranging, the solution of (63) can be derived as

$$I_A = \frac{2}{d^m} \left(\frac{m}{\bar{\gamma}}\right)^m e^{-\frac{\lambda}{2}} \sum_{n=u}^{\infty} \left(\frac{\lambda}{2}\right)^n \frac{1}{\Gamma(n+1)} \times {}_1F_1\left(m; 1+n; \frac{\lambda}{2d}\right), \tag{66}$$

where $d = \frac{\bar{\gamma}+m}{\bar{\gamma}}$.

*2) Evaluating $I_B$ in (62):* Simplifying and rearranging (62), we derive

$$I_B = \frac{2}{\Gamma(m)} \left(\frac{m}{\bar{\gamma}}\right)^m e^{-\frac{\lambda}{2}} \sum_{n=u}^{\infty} \left(\frac{\lambda}{2}\right)^{\frac{n}{2}} \int_0^{\infty} \gamma^{m-\frac{n}{2}-1} e^{-d\gamma} \times I_n\left(\sqrt{2\lambda\gamma}\right) Q_m\left(\sqrt{2a\rho\gamma}, \sqrt{2a\gamma}\right) \mathrm{d}\gamma. \tag{67}$$

Using (54) with simplification and rearranging, we write (67) as

$$I_B = \frac{2}{\Gamma(m)} \left(\frac{m}{\bar{\gamma}}\right)^m e^{-\frac{\lambda}{2}} \sum_{n=u}^{\infty} \sum_{i=0}^{\infty} \sum_{k=0}^{i+m-1} \left(\frac{\lambda}{2}\right)^{\frac{n}{2}} \frac{a^{i+k}\rho^i}{i!k!} \times \int_0^{\infty} \gamma^{m-\frac{n}{2}+i+k-1} e^{-\gamma c} \mathrm{d}\gamma, \tag{68}$$

where $c = 1 + a(\rho+1) + \frac{m}{\bar{\gamma}}$. Similarly, implementing same procedures as (66), the solution of (68) can be given as

$$I_B = \frac{2}{\Gamma(m)} \left(\frac{m}{\bar{\gamma}}\right)^m e^{-\frac{\lambda}{2}} \sum_{n=u}^{\infty} \sum_{i=0}^{\infty} \sum_{k=0}^{i+m-1} \left(\frac{\lambda}{2}\right)^n \frac{a^{i+k}\rho^i}{i!\,k!} \times \frac{\Gamma(m+i+k)}{\Gamma(n+1)\,c^{m+i+k}} {}_1F_1\left(m+i+k; 1+n; \frac{\lambda}{2c}\right). \tag{69}$$

Substituting (66) and (69) into (60), this concludes the derivation.

## APPENDIX D
## EXPRESSION FOR TRIPLE SC

In this section, we drive (28). Using (53) and substituting (20) into (9), we drive the average probability of detection as

$$\overline{P}_{D,SC,3} = \frac{\left|\mathbf{\Sigma}^{-1}\right|^m}{\Gamma(m)} e^{-\frac{\lambda}{2}} \sum_{n=0}^{\infty} \sum_{k=0}^{n+u-1} \sum_{i=0}^{\infty} \sum_{j=0}^{\infty} \times \frac{\left|p_{1,2}\right|^{2i} \left|p_{2,3}\right|^{2j} \left(\frac{\lambda}{2}\right)^k}{p_{1,1}^{i+m} p_{2,2}^{i+j+m} p_{3,3}^{j+m} \Gamma(m+i)\Gamma(m+j)\, i!\, j!\, k!\, n!} \times \underbrace{\int_0^{\infty} \gamma^n e^{-\gamma} \left[\Theta_1+\Theta_2+\Theta_3\right] \mathrm{d}\gamma}_{I_A}. \tag{70}$$

Substituting (21), (22) and (23) into (70), the integral part $I_A$ in (70) becomes

$$I_A = \left(\frac{p_{1,1}\, m}{\bar{\gamma}}\right)^{i+m} I_{a1} + \left(\frac{p_{2,2}\, m}{\bar{\gamma}}\right)^{i+j+m} I_{a2} + \left(\frac{p_{3,3}\, m}{\bar{\gamma}}\right)^{j+m} I_{a3}, \tag{71}$$

where

$$I_{a1} = \int_0^{\infty} \gamma^{i+m+n-1} e^{-\gamma\left(\frac{p_{1,1} m}{\bar{\gamma}}+1\right)} \times \gamma\left(i+j+m, \frac{p_{2,2}\, m}{\bar{\gamma}}\gamma\right) \gamma\left(j+m, \frac{p_{3,3}\, m}{\bar{\gamma}}\gamma\right) \mathrm{d}\gamma. \tag{72}$$

$$I_{a2} = \int_0^{\infty} \gamma^{i+j+m+n-1} e^{-\gamma\left(\frac{p_{2,2}\, m}{\bar{\gamma}}+1\right)} \times \gamma\left(i+m, \frac{p_{1,1}\, m}{\bar{\gamma}}\gamma\right) \gamma\left(j+m, \frac{p_{3,3}\, m}{\bar{\gamma}}\gamma\right) \mathrm{d}\gamma. \tag{73}$$

$$I_{a3} = \int_0^{\infty} \gamma^{j+m+n-1} e^{-\gamma\left(\frac{p_{3,3}\, m}{\bar{\gamma}}+1\right)} \times \gamma\left(i+m, \frac{p_{1,1}\, m}{\bar{\gamma}}\gamma\right) \gamma\left(i+j+m, \frac{p_{2,2}\, m}{\bar{\gamma}}\gamma\right) \mathrm{d}\gamma. \tag{74}$$

Each integral in (71) could be written as

$$I = \int_0^{\infty} x^a e^{-bx} \gamma\left(d_1, c_1 x\right) \gamma\left(d_2, c_2 x\right) \mathrm{d}x. \tag{75}$$

Using [[30], Eq. (10)], we write (71) as

$$I_A = \left(\frac{\bar{\gamma}}{m}\right)^n \frac{p_{1,1}^{i+m} p_{2,2}^{i+j+m} p_{3,3}^{j+m} \Gamma(2i+2j+3m+n)}{\left(p_{11}+p_{2,2}+p_{3,3}+\frac{\bar{\gamma}}{m}\right)^{(2i+2j+3m+n)}} \times \left(\Xi_1+\Xi_2+\Xi_3\right), \tag{76}$$

where $\Xi_1$, $\Xi_2$ and $\Xi_3$ are in (25), (26) and (27), respectively. Substituting (76) into (70), this concludes the derivations.

## Appendix E
## General Expression for Triple SC

In this section, we derive the expression in (29). Using (52) and substituting (20) into (9) we derive

$$\overline{P}_{D,SC,3} = \frac{\left|\mathbf{\Sigma}^{-1}\right|^m}{\Gamma(m)} \sum_{n=0}^{\infty}\sum_{i=0}^{\infty}\sum_{j=0}^{\infty} \frac{\Gamma\big(u+n,\frac{\lambda}{2}\big)}{\Gamma(u+n)} \times \frac{\left|p_{1,2}\right|^{2\,i}\,\left|p_{2,3}\right|^{2\,j}}{p_{1,1}^{i+m} p_{2,2}^{i+j+m} p_{3,3}^{j+m} \Gamma(m+i)\,\Gamma(m+j)\,i!\,j!\,n!} \times \underbrace{\int_0^{\infty} \gamma^n\, e^{-\gamma}\left[\Theta_1+\Theta_2+\Theta_3\right]\mathrm{d}\gamma}_{I_A}. \quad (77)$$

Following same procedures in (71)-(76), then substituting (76) into (77), this concludes the derivation.

## Appendix F
## Expression for Dual SSC

In this section, we will derive the expression in (37) by evaluating $\overline{P}_{D,SSC,2}$ in (32) as follows.

*1) Integral $I_A$ in (33):* Using Marcum Q-function alternative representation (53), we rewrite (33) as

$$I_A = 2\,e^{-\frac{\lambda}{2}} \sum_{j=0}^{\infty}\sum_{k=0}^{j+u-1} \left(\frac{\lambda}{2}\right)^k \frac{1}{j!\,k!} \times \int_0^{\infty} \gamma^{j+m-1} \exp\left\{-\gamma(1+\frac{m}{\bar{\gamma}})\right\}\mathrm{d}\gamma. \quad (78)$$

Using (56) and satisfying the condition therein, we solve (78) as

$$I_A = 2\,e^{-\frac{\lambda}{2}} \sum_{j=0}^{\infty}\sum_{k=0}^{j+u-1} \left(\frac{\lambda}{2}\right)^k \frac{(j+m-1)!}{j!\,k!} \left(\frac{\bar{\gamma}}{\bar{\gamma}+m}\right)^{j+m}. \quad (79)$$

*2) Integral $I_B$ in (34):* Following the same procedures as in (78), we rewrite (34) as

$$I_B = e^{-\frac{\lambda}{2}} \sum_{n=0}^{\infty}\sum_{q=0}^{j+u-1}\sum_{i=0}^{\infty}\sum_{k=0}^{i+m-1} \left(\frac{\lambda}{2}\right)^q \frac{a^{i+k}\,\rho^i}{i!\,k!\,n!\,q!} e^{-a\,\gamma_T}\,\gamma_T^k \times \int_0^{\infty} \gamma^{m+n+i-1} \exp\left\{-\gamma\left(a\,\rho+\frac{m}{\bar{\gamma}}+1\right)\right\}\mathrm{d}\gamma. \quad (80)$$

Similarly as we did in (79), we solve (80) as

$$I_B = e^{-\frac{\lambda}{2}} \sum_{n=0}^{\infty}\sum_{q=0}^{j+u-1}\sum_{i=0}^{\infty}\sum_{k=0}^{i+m-1} \left(\frac{\lambda}{2}\right)^q \frac{a^{i+k}\,\rho^i}{i!\,k!\,n!\,q!} \times \frac{(m+n+i-1)!}{\left(a\,\rho+\frac{m}{\bar{\gamma}}+1\right)^{m+n+i}} e^{-a\,\gamma_T}\,\gamma_T^k. \quad (81)$$

*3) Integral $I_C$ in (35):* Using (53), we rewrite (35) as

$$I_C = e^{-\frac{\lambda}{2}} \sum_{n=0}^{\infty}\sum_{q=0}^{n+u-1} \frac{1}{n!\,q!}\left(\frac{\lambda}{2}\right)^k \times \int_0^{\gamma_T} \gamma^{m+n-1} \exp\left\{-\gamma\left(\frac{m}{\bar{\gamma}}+1\right)\right\}\mathrm{d}\gamma. \quad (82)$$

Using [[18], Eq. (3.351/1)], where

$$\int_0^z x^n e^{-\mu\,x}\mathrm{d}x = \frac{n!}{\mu^{n+1}} - e^{-\mu z}\sum_{k=0}^{n}\frac{n!}{k!}\frac{z^k}{\mu^{n-k+1}} = \mu^{-n-1}\gamma(n+1,\mu z), \quad \left[z>0, \mathrm{Re}\,\mu>0,\, n=0,\,1,\,2,\cdots\right], \quad (83)$$

we derive (82) as

$$I_C = e^{-\frac{\lambda}{2}} \sum_{n=0}^{\infty}\sum_{q=0}^{n+u-1} \frac{1}{n!\,q!}\left(\frac{\lambda}{2}\right)^q \left(\frac{\bar{\gamma}}{\bar{\gamma}+m}\right)^{m+n} \times\gamma\left(m+n,\gamma_T\left(\frac{\bar{\gamma}+m}{\bar{\gamma}}\right)\right). \quad (84)$$

Substituting (79), (80) and (84) into (32), this concludes the derivation.

## Appendix G
## Alternative Expression for Dual SSC

In this section, we will derive the expression in (38) by evaluating $\overline{P}_{D,SSC,2}$ in (32) for alternative expression as follows.

*1) Integral $I_A$ in (33):* Let $x=\sqrt{2\,\gamma}$ , we rewrite (33) as

$$I_A = \frac{4}{2^{-m}}\int_0^{\infty} Q_u\left(x,\sqrt{\lambda}\right) x^{m-1}\exp\left(-\frac{m\,x^2}{2\bar{\gamma}}\right)\mathrm{d}x. \quad (85)$$

Using [[31], Eq. (8)], we solve (85) as

$$I_A = 4\sum_{j=0}^{\infty}\frac{\Gamma(m+j)\Gamma\big(u+j,\frac{\lambda}{2}\big)}{\Gamma(u+j)\left(1+\frac{m}{\bar{\gamma}}\right)^{m+j} j!}. \quad (86)$$

*2) Integral $I_B$ in (34):* Using (52) and (53) for $Q_u\left(\sqrt{2\,\gamma},\,\sqrt{\lambda}\right)$ and $Q_m\left(\sqrt{2\,a\,\rho\,\gamma},\,\sqrt{2\,a\,\gamma_T}\right)$, we rewrite (34) as

$$I_B = \sum_{n=0}^{\infty}\sum_{i=0}^{\infty}\sum_{k=0}^{i+m-1} \frac{\Gamma\big(u+n,\frac{\lambda}{2}\big)}{\Gamma(u+n)\;n!}\frac{a^{i+k}\,\rho^i}{i!\,k!}\,\gamma_T^k\,e^{-a\,\gamma_T} \times\int_0^{\infty}\gamma^{m+n+i-1}\,e^{-\gamma\,\left(\frac{m}{\bar{\gamma}}+a\,\rho+1\right)}\,\mathrm{d}\gamma. \quad (87)$$

Using (56) , we solve (87) as

$$I_B = \sum_{n=0}^{\infty}\sum_{i=0}^{\infty}\sum_{k=0}^{i+m-1} \frac{\Gamma\big(u+n,\frac{\lambda}{2}\big)\Gamma(m+n+i)}{\Gamma\left(u+n\right)\left(\frac{m}{\gamma}+a\rho+1\right)^{m+n+i} n!\,i!\,k!} \times a^{i+k}\rho^i\gamma_T^k e^{-a\gamma_T}. \quad (88)$$

*3) Integral $I_C$ in (35):* Using (52), we rewrite (35) as

$$I_C = \sum_{p=0}^{\infty} \frac{\Gamma\big(u+p, \frac{\lambda}{2}\big)}{\Gamma(u+p)\; p!} \int_0^{\gamma_T} \gamma^{m+p-1}\, e^{-\gamma\left(\frac{\bar{\gamma}+m}{\bar{\gamma}}\right)}\, \mathrm{d}\gamma. \tag{89}$$

Using (83), we solve (89) for $m$ integer values as

$$\begin{aligned} I_C = &\sum_{p=0}^{\infty} \frac{\Gamma\big(u+p, \frac{\lambda}{2}\big)}{\Gamma(u+p)\; p!} \left(\frac{\bar{\gamma}+m}{\bar{\gamma}}\right)^{-(m+p)} \\ &\times \gamma\left(m+p, \gamma_T \left(\frac{\bar{\gamma}+m}{\bar{\gamma}}\right)\right). \end{aligned} \tag{90}$$

Substituting (86), (88) and (90) into (32), this concludes the derivation.

## Appendix H
## Expression for Optimal Threshold

In this section, we will derive the expression in (39). Employing Leibniz's rule [[19], Eq. (3.3.7)] with the aid of following identity given in [[29], Eq. (9)] as

$$\frac{\partial}{\partial \beta} Q_u\left(\alpha, \beta\right) = -\beta \left(\frac{\beta}{\alpha}\right)^{u-1} \exp\left(-\frac{\alpha^2+\beta^2}{2}\right) I_{u-1}\left(\alpha\, \beta\right), \tag{91}$$

we rewrite (32) as

$$\begin{aligned} \frac{\partial}{\partial \gamma_T^*} \overline{P}_{D,SSC,2} = &\frac{1}{\Gamma(m)} \left(\frac{m}{\bar{\gamma}}\right)^m \Bigg[\rho^{\frac{1-m}{2}} \sqrt{2a}\, {\gamma_T^*}^{1-\frac{m}{2}}\, e^{-a\gamma_T^*} \\ &\times \underbrace{\int_0^{\infty} Q_u\left(\sqrt{2\,\gamma},\, \sqrt{\lambda}\right) \gamma^{\frac{m-1}{2}}\, e^{-a\gamma} I_{m-1}\left(2a\sqrt{\rho\gamma_T^*\gamma}\right) \mathrm{d}\gamma}_{I} \\ &- Q_u\left(\sqrt{2\,\gamma_T^*},\, \sqrt{\lambda}\right) {\gamma_T^*}^{m-1} \exp\left(-\frac{m\,\gamma_T^*}{\bar{\gamma}}\right)\Bigg]. \end{aligned} \tag{92}$$

To solve the integral $I$ in (92), we perform changing variable along with the aid of the series expansion of the modified Bessel function given in [[18], Eq. (8.445)] as

$$I_\nu\left(z\right) = \sum_{k=0}^{\infty} \frac{1}{\Gamma(\nu+k+1)\, k!} \left(\frac{z}{2}\right)^{\nu+2\,k}. \tag{93}$$

Then, we drive (92) as

$$\begin{aligned} \frac{\partial}{\partial \gamma_T^*} \overline{P}_{D,SSC,2} = &\frac{1}{\Gamma(m)} \left(\frac{m}{\bar{\gamma}}\right)^m \Bigg[\rho^{\frac{1-m}{2}} \sqrt{2a\, \gamma_T^*} e^{-a\gamma_T^*} \\ &\times \sum_{k=0}^{\infty} \frac{1}{\Gamma(m+k) 2^{m+k}\, k!} \left(a\sqrt{\rho}\right)^{m+2k-1} {\gamma_T^*}^{k} \\ &\times \underbrace{\int_0^{\infty} Q_u\left(x, \sqrt{\lambda}\right) x^{2(m+k)-1} e^{-\frac{a}{2}x^2} \mathrm{d}x}_{I} \\ &- Q_u\left(\sqrt{2\,\gamma_T^*},\, \sqrt{\lambda}\right) {\gamma_T^*}^{m-1} \exp\left(-\frac{m\,\gamma_T^*}{\bar{\gamma}}\right)\Bigg]. \end{aligned} \tag{94}$$

Using [[29], Eq. (29)] by following same procedures as in (50), we can solve the integral $I$ in (94) as

$$\begin{aligned} I_A = &G_1^{'} + \frac{1}{2} \sum_{n=1}^{u-1} \left(\frac{\lambda}{2}\right)^n \frac{\Gamma\left(m+k\right)}{\left(\frac{a+1}{2}\right)^{m+k} n!} \\ &\times {}_1F_1\left(m+k; n+1; \frac{\lambda}{2\,(a+1)}\right), \end{aligned} \tag{95}$$

where $G_1^{'}$ can be obtained by evaluating the following integral containing the first order of Marcum $Q$-function $Q(.,.)$ for integer $m$ values as

$$G_1^{'} = \int_0^{\infty} Q\left(x, \sqrt{\lambda}\right) x^{2(m+k)-1}\, e^{-\frac{a}{2}x^2}\, \mathrm{d}x. \tag{96}$$

Using [[29], Eq. (25)], we evaluate $G_1^{'}$ for integer $m$ values as

$$\begin{aligned} G_1^{'} = &\frac{2^{m+k-1}\left(m+k-1\right)!}{a^{2(m+k)}} \left(\frac{1}{a+1}\right) e^{-\frac{\lambda}{2}\,\frac{a}{a+1}} \\ &\times \Bigg[\left(1+a\right)\left(\frac{a}{1+a}\right)^{m+k-1} L_{m+k-1}\left(-\frac{\lambda}{2\left(1+a\right)}\right) \\ &+ \sum_{n=0}^{m+k-2} \left(\frac{a}{a+1}\right)^n L_n\left(-\frac{\lambda}{2\left(a+1\right)}\right)\Bigg], \end{aligned} \tag{97}$$

where $L_n\left(.\right)$ denotes Laguerre polynomial of $n$-degree [18]. Substituting (95) into (94), this concludes the derivation.

## References


[1] H. Urkowitz, "Energy detection of unknown deterministic signals," *Proceedings of the IEEE*, vol. 55, no. 4, pp. 523–531, Apr. 1967.

[2] M.-S. Alouini and M. K. Simon, "Multichannel reception of digital signals over correlated nakagami fading channels," in *Proc. of the Annual Allerton Conf. on Commun. Control and Computing*, vol. 36. Citeseer, 1998, pp. 146–155.

[3] M. K. Simon and M.-S. Alouini, "Digital communication over fading channels," *JOHN WILEY and SONS, INC,2005*, 2005,ISBN 0-471-20069-7.

[4] S. Al-Juboori and X. Fernando, "Unified approach for performance analysis of cognitive radio spectrum sensing over correlated multipath fading channels," in *WoWMoM, 2015 IEEE 16th Int. Symposium*. IEEE, Boston, USA, 2015, pp. 1–6.

[5] ——, "Multi-antenna spectrum sensing over correlated nakagami-m channels with mrc and egc diversity receptions," *IEEE Transactions on Vehicular Technology*, 2017.

[6] ——, "Correlated multichannel spectrum sensing cognitive radio system with selection combining," in *2016 IEEE Global Commun. Conf. (GLOBECOM)*, Dec 2016, pp. 1–6.

[7] V. Kostylev, "Energy detection of a signal with random amplitude," in *IEEE Int. Conf. on Commun., ICC 2002.*, vol. 3, Apr-May 2002, pp. 1606–1610 vol.3.

[8] F. Digham, M.-S. Alouini, and M. K. Simon, "On the energy detection of unknown signals over fading channels," in *Commun., 2003. ICC '03. IEEE Int. Conf.*, vol. 5, May 2003, pp. 3575–3579 vol.5.

[9] ——, "On the energy detection of unknown signals over fading channels," *Commun., IEEE Trans. on*, vol. 55, no. 1, pp. 21–24, Jan. 2007.

[10] S. P. Herath, N. Rajatheva, and C. Tellambura, "On the energy detection of unknown deterministic signal over nakagami channels with selection combining," in *Canadian Conf. on Electrical and Computer Engineering, 2009. CCECE'09.* IEEE, 2009, pp. 745–749.

[11] S. Herath, N. Rajatheva, and C. Tellambura, "Energy detection of unknown signals in fading and diversity reception," *IEEE Trans. on Commun.*, vol. 59, no. 9, pp. 2443–2453, Sept. 2011.

[12] A. Shahini, A. Bagheri, and A. Shahzadi, "A unified approach to performance analysis of energy detection with diversity receivers over nakagami-m fading channels," in *2013 Int. Conf. on Connected Vehicles and Expo (ICCVE)*. IEEE, 2013, pp. 707–712.

[13] Y. Zeng and Y.-C. Liang, "Spectrum-sensing algorithms for cognitive radio based on statistical covariances," *IEEE trans. on Vehicular Technology*, vol. 58, no. 4, pp. 1804–1815, 2009.

[14] A. Patel, Z. Khan, S. Merchant, U. Desai, and L. Hanzo, "The achievable rate of interweave cognitive radio in the face of sensing errors," *IEEE Access*, vol. PP, no. 99, pp. 1–1, 2016.

[15] A. Annamalai, O. Olabiyi, S. Alam, O. Odejide, and D. Vaman, "Unified analysis of energy detection of unknown signals over generalized fading channels," in *Wireless Commun. and Mobile Computing Conf. (IWCMC), 2011 7th Int.* IEEE, 2011, pp. 636–641.

[16] M. Nakagami, "The m-distribution-a general formula of intensity distribution of rapid fading," *Statistical Method of Radio Propagation*, 1960.

[17] G. Fedele, L. Izzo, and M. Tanda, "Dual diversity reception of m-ary dpsk signals over nakagami fading channels," in *Personal, Indoor and Mobile Radio Commun., 1995. PIMRC'95. Wireless: Merging onto the Information Superhighway., Sixth IEEE Int. Symposium on*, vol. 3, Sept 1995, pp. 1195–1201.

[18] I. Gradshteyn and I. Ryzhik, "*Table of Integrals, Series and Products*," *Alan Jeffrey and Daniel Zwillinger (eds.), Seventh edition (Feb 2007)*, p. 885, 2007.

[19] M. Abramowitz and I. A. Stegun, *Handbook of mathematical functions: with formulas, graphs, and mathematical tables*. Courier Dover Publications, 1972, no. 55.

[20] C. C. Tan and N. C. Beaulieu, "Infinite series representations of the bivariate rayleigh and nakagami-m distributions," *Commun., IEEE Trans. on*, vol. 45, no. 10, pp. 1159–1161, 1997.

[21] S. Gaur and A. Annamalai, "Some Integrals involving the $Q_m\left(a\sqrt{x}, b\sqrt{x}\right)$ with application to error probability analysis of diversity receivers," *IEEE transactions on vehicular technology*, vol. 52, no. 6, pp. 1568–1575, 2003.

[22] G. Cui, L. Kong, X. Yang, and D. Ran, "Two useful integrals involving generalised marcum q-function," *Electronics letters*, vol. 48, no. 16, pp. 1017–1018, 2012.

[23] N. Y. Ermolova and O. Tirkkonen, "Laplace transform of product of generalized marcum q, bessel i, and power functions with applications." *IEEE Trans. Signal Processing*, vol. 62, no. 11, pp. 2938–2944, 2014.

[24] P. C. Sofotasios, S. Muhaidat, G. K. Karagiannidis, and B. S. Sharif, "Solutions to integrals involving the marcum q-function and applications," *IEEE Signal Processing Letters*, vol. 22, no. 10, pp. 1752–1756, 2015.

[25] K. Cao and X. Gao, "Solutions to generalized integrals involving the generalized marcum q-function with application to energy detection," *IEEE Communications Letters*, vol. 20, no. 9, pp. 1780–1783, 2016.

[26] G. K. Karagiannidis, D. Zogas, S. Kotsopoulos *et al.*, "An efficient approach to multivariate nakagami-m distribution using green's matrix approximation," *Wireless Commun., IEEE Trans.*, vol. 2, no. 5, pp. 883–889, 2003.

[27] V. A. Aalo, "Performance of maximal-ratio diversity systems in a correlated nakagami-fading environment," *IEEE Trans. on Commun.,*, vol. 43, no. 8, pp. 2360–2369, 1995.

[28] N. M. Temme, "Computational aspects of incomplete gamma functions with large complex parameters," in *Approximation and Computation: A Festschrift in Honor of Walter Gautschi*. Springer, 1994, pp. 551–562.

[29] A. H. Nuttall, "Some integrals involving the q-function," DTIC Document, Tech. Rep., 1974.

[30] G. K. Karagiannidis, D. A. Zogas, and S. A. Kotsopoulos, "Performance analysis of triple selection diversity over exponentially correlated nakagami-m fading channels," *Commun., IEEE Trans.*, vol. 51, no. 8, pp. 1245–1248, 2003.

[31] P. C. Sofotasios, M. Valkama, T. A. Tsiftsis, Y. A. Brychkov, S. Freear, and G. K. Karagiannidis, "Analytic solutions to a marcum q-function-based integral and application in energy detection of unknown signals over multipath fading channels," in *9th Int. Conf. on Cognitive Radio Oriented Wireless Networks and Commun. (CROWNCOM), 2014*. IEEE, 2014, pp. 260–265.